

Article

Effects of TiO₂ Nanoparticle Addition on Microstructure and Selected Properties of Ag–xTiO₂ Composites

Anna Wąsik ¹, Beata Leszczyńska-Madej ^{1,*}  and Marcin Madej ² 

¹ Department of Materials Science and Non Ferrous Metals Engineering, Faculty of Non Ferrous Metals, AGH University of Science and Technology, 30 Mickiewicza Ave., 30059 Cracow, Poland; anna.wasik@agh.edu.pl

² Department of Physical and Powder Metallurgy, Faculty of Metals Engineering and Industrial Computer Science, AGH University of Science and Technology, 30 Mickiewicza Ave., 30059 Cracow, Poland; mmadej@agh.edu.pl

* Correspondence: bleszcz@agh.edu.pl; Tel.: +48-126-173-573

Abstract: The paper presents the results of a study of the microstructure and selected properties of silver-based composites reinforced with TiO₂ nanoparticles, produced by the powder metallurgy method. Pure silver powders were mixed with TiO₂ reinforcement (5 and 10 wt%) and 5 mm steel balls (100Cr6) for 270 min in a Turbula T2F mixer to produce a homogeneous mixture. The composites were made in a rigid die with a single-action compaction press under a pressure of 400 MPa and 500 MPa and then sintered under nitrogen atmosphere at 900 °C. Additionally, to improve the density and mechanical properties of the obtained sinters, double pressing and double sintering operations were conducted. As a result, compacts with a density of 90–94% were obtained. The microstructure of the sintered compacts consists of uniform grains, and the TiO₂ reinforcement phase particles are located on the grain boundaries. There were no discontinuities at the Ag–TiO₂ contact boundary, which was confirmed by SEM and TEM analysis. The use of a higher pressure had a positive effect on the hardness and flexural strength of the tested materials. It was found that the composites with 5 wt% TiO₂ pressed under 500 MPa are characterized by the highest level of mechanical properties. The hardness of these composites is 57 HB, while the flexural strength is 163 MPa.

Keywords: Ag–xTiO₂ composites; powder metallurgy; microstructure investigations; silver; TiO₂ nanoparticles



Citation: Wąsik, A.; Leszczyńska-Madej, B.; Madej, M. Effects of TiO₂ Nanoparticle Addition on Microstructure and Selected Properties of Ag–xTiO₂ Composites. *Materials* **2021**, *14*, 4846. <https://doi.org/10.3390/ma14174846>

Academic Editors: Tomasz Tański and Przemysław Snopiński

Received: 3 August 2021

Accepted: 23 August 2021

Published: 26 August 2021

Publisher's Note: MDPI stays neutral with regard to jurisdictional claims in published maps and institutional affiliations.



Copyright: © 2021 by the authors. Licensee MDPI, Basel, Switzerland. This article is an open access article distributed under the terms and conditions of the Creative Commons Attribution (CC BY) license (<https://creativecommons.org/licenses/by/4.0/>).

1. Introduction

Metal–ceramic composites have attracted much attention due to their extraordinary properties such as high strength, low weight, high fatigue strength or electrical properties when compared to traditional materials [1,2]. However, the final properties of the composite material are greatly affected by the method of manufacturing, component composition and weight/volume fraction of individual components and, in particular, depend on the amount and size of the introduced reinforcement particles since it is the size of the particles that determines the reinforcement mechanism [3]. Pure silver is an excellent conductor of heat and electricity [4]; nonetheless, introducing reinforcing particles affects its thermal conductivity. Wiczeorek et al. [5] showed that the presence of a reinforcing phase in the form of Al₂O₃ and SiC particles leads to a decrease in the thermal conductivity in relation to pure silver. Silver is also characterized by high plasticity, ductility and chemical durability [6]. To improve its strength properties and wear resistance, reinforcing phase particles are introduced into the silver matrix [7]. For example, Rigou et al. [8], in their study, added diamond particles as suspension to the plating silver bath to improve the sliding wear behavior of silver-plated surfaces, which are normally characterized by low hardness and poor wear resistance. The results show that the surface of the silver coating containing diamond particles exhibited low values of the coefficient of friction and wear rate.

Silver matrix composites can be classified according to the type of dispersed phase, which may be a pure element or carbide and oxides. Very common reinforcement particles for silver matrix composites are oxides such as CdO, SnO₂, ZnO, Al₂O₃ and TiO₂ [9]. Among them, TiO₂ has attracted great attention as a reinforcing phase due to its high chemical stability and low cost [10]. The application of TiO₂ particles as a reinforcement increases the hardness, wear and corrosion resistance of the base material [11,12]. However, to fulfill its function properly, the reinforcement phase has to be homogeneously distributed in the matrix material. Haoa et al. [13] fabricated a silver matrix composite reinforced with Ag-doped graphene nanosheets using powder metallurgy methods. Their results indicate that the silver matrix composite, due to the homogeneous dispersion of Ag-doped graphene, has good comprehensive properties at 0.5 wt% Ag-doped graphene, in which electrical conductivity reaches up to 98.62% IACS. Thanks to the mentioned properties, silver matrix composites have found application in the electronic packing industry as contact materials in electronics and electrical brushes [14–16].

Silver, additionally, has antimicrobial and photocatalytic activity; therefore, it has found its use in biomedical applications [17]. The antibacterial properties of composites with a silver matrix have also been tested by many authors. Yen-Wen Wanga et al. [18] obtained macroporous Ag–TiO₂ composite foams which exhibited strong antibacterial activity against *Escherichia coli* bacteria. The antibacterial activity of silver matrix composites makes them a material suitable for antibacterial and photocatalytic activities that can be successfully used in chemical filtration applications. Nanocomposite systems with high photoactivity, such as silver-modified TiO₂, are employed as electrodes for dye degradation [19,20]. Youngmi Koo et al. [21], in their research, indicate that Ag–TiO₂–CNT composite nanoparticles can be used in environmental protection as a factor enabling the breakdown of organic pollutants.

Robert Liang et al. [22] investigated the alternative application of Ag–TiO₂ thin film composites in the photocathodic protection of stainless steel, while improving the degradation of pollutants under photocatalysis. The authors noted that corrosion in moist chloride-containing environments is still a concern as the passive film formed on the surface of stainless steel is broken down. A potential solution to this problem is photocathodic protection. TiO₂ is commonly used as a photoanode material [23]. However, the authors indicated that it requires ultraviolet light and rapidly undergoes charge re-combination. Therefore, metal nanoparticles, such as silver, might be added. In the above-mentioned work [22], the authors deposited Ag nanoparticles in a silica–titanium coating with the addition of TiO₂ onto glass by electrophoretic deposition. This solution allowed minimization of the weight loss as a result of corrosion processes and surface oxidation.

As was mentioned above, manufacturing methods have a significant effect on the final properties of composite materials as they have to provide uniform distribution of the reinforcement in the matrix material. Various methods can be used to produce metal matrix composites and may be based on casting methods or the powder metallurgy technique [24]. This study thus investigated the effect of a TiO₂ nanoparticle addition on the densification, microstructure and selected properties of Ag–xTiO₂ composites prepared by conventional powder metallurgy techniques. Particular attention was paid to the interface of the Ag matrix and the reinforcement phase as well as to the phenomena occurring in the material during the manufacturing process, including the stability of the TiO₂ phase.

2. Materials and Methods

The research material was electrolytic silver powders with a particle size below 63 µm and TiO₂ nanopowders (anatase, particle size below 100 nm). The use of metal powders results in a larger specific surface area and, thus, in the case of silver, it allows greater release of silver ions and easier interaction with other particles, while providing better antimicrobial properties, which is an important factor when using these composites in antibacterial activities. Mixtures containing 5 wt% and 10 wt% TiO₂ were prepared from the powders. Figure 1 below shows micrographs of the Ag and TiO₂ powder particles and

the Ag + 10 wt% TiO₂ mixture. Silver powder has a dendritic and partially irregular shape, while TiO₂ powder forms agglomerates composed of particles with a nearly spherical shape already at the stage of storage. In order to break the TiO₂ clusters, mixing with the participation of balls was used, which resulted in a change in the shape and “spinning” of the silver powder particles. As a result of mixing in the Turbula T2F mixer with the participation of balls, a homogeneous mixture was obtained; the TiO₂ particles are evenly distributed on the surface of the silver particles and do not form clusters. The parameters of the milling process were as follows: balls 5 mm in diameter, 100Cr6 heat-treated steel (about 50 HRC); milling time 270 min, input (milling media + mixture) was 40% of the milling cup volume; the ratio of the balls to the milled powder was 2:1.

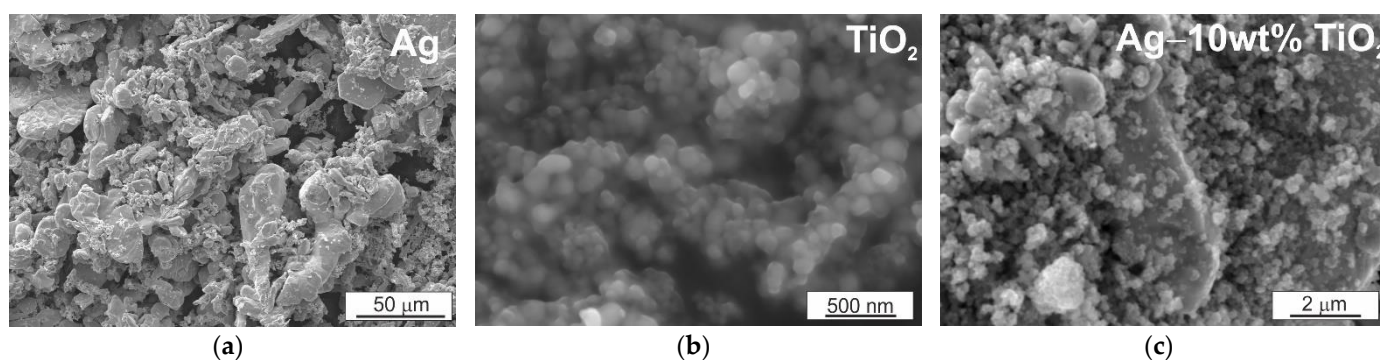


Figure 1. Powder morphology: (a) Ag (0–63 μm); (b) nano TiO₂; (c) Ag–10 wt% TiO₂; SEM.

The composites were produced in a single-action compaction press followed by sintering under nitrogen atmosphere at 900 °C for 1 h. Pressures of 400 MPa and 500 MPa were used for pressing, no lubricants were used, and they were cold pressed. In order to increase the density of the composites, the pressing operation was conducted at the same pressure and the samples were successively sintered under nitrogen atmosphere at the temperature of 650 °C for 1 h. The secondary pressing process was used to improve the density of the tested materials, the density of which after the first pressing was not sufficient. The second sintering is treated more as a procedure of eliminating internal stresses and recrystallization with a possible increase in the contact surface between the particles as a result of diffusion processes. The TiO₂ reinforcement phase was added in amounts of 5 wt% and 10 wt%. Samples with dimensions of 4 × 5 × 40 mm were produced. The scheme of Ag–xTiO₂ composite manufacturing process is presented in Figure 2.

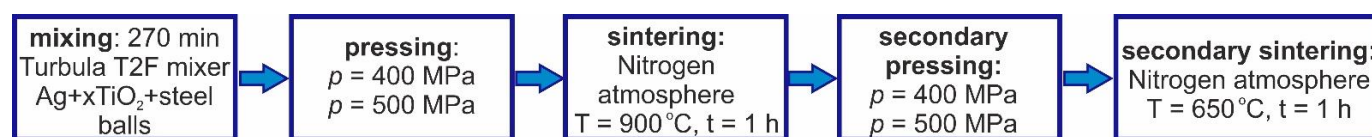


Figure 2. Scheme of Ag–xTiO₂ composite manufacturing process.

Microstructure studies were carried out on the sinters made in this way using a Hitachi Su 70 scanning electron microscope (Hitachi, Tokyo, Japan). The micrographs were taken during operation of the detector collecting secondary electrons (SE) or backscattered electrons (BSE). Additionally, the chemical composition was analyzed using the wavelength-dispersive X-ray spectroscopy (WDS) method (Thermo Fisher Scientific, Waltham, MA, USA) and the phase composition was analyzed using a BRUKER X-ray diffractometer with a Co K α = 0.179 nm (1.79 Å) cobalt lamp (D8 Advance, Bruker, Karlsruhe, Germany). Observations of the microstructure of the samples in the submicron range were made using a JEOL JEM-2010 ARP transmission electron microscope (Jeol Ltd., Tokyo, Japan). The specimens for observation were prepared by the ion thinning method using a Precision Ion Polishing System (PIPS) device by Gatan (Gatan, Inc., Pleasanton, CA, 94588, USA).

Hardness measurements were made by the Brinell method employing an INNOVATEST hardness tester (Innovatest BV, Maastricht, The Netherlands). A tungsten carbide ball with a diameter of 2.5 mm was used and measurements were made with a load of 62.5 kg. Each sample was measured at five places, whereby a distance of at least two impression diameters was kept between the impressions. The flexural strength test was carried out using the three-point bending method on a Zwick Roell Z020 testing machine (Zwick AG, Ulm, Germany). The test was carried out in accordance with the PN EN ISO 7438 standard. The crosshead speed was 0.05 mm/s.

3. Results and Discussion

The final density of the composites largely depends on the first pressing pressure used, in addition to the proportion of TiO_2 addition. A critical step in the pressing of silver-based materials in a multi-stage process is the first pressing; the second one only slightly changes or eliminates the swelling effect during the first sintering. Due to its hard nature, the addition of TiO_2 makes the pressing process difficult, even if it has been successfully distributed on the surface of the silver particles by milling. Powder mixtures composed of two or more components exhibit poorer compatibility and formability than pure metals. The sintering of silver is a critical step in the entire manufacturing process of finished products owing to its tendency to swell during this process. In the studied materials, the TiO_2 addition is evenly distributed in the sample, which makes it difficult to close the pores already at the pressing stage by creating a network of channels that allow the gas to move in the sintering atmosphere and, thus, prevent its pressure from increasing in the closed pores inside the sinter. As a result, it was possible to obtain a final sintered density at the level of about or higher than 90% for the samples that were pressed with the first pressure of 500 MPa. The graph presented in Figure 3 clearly shows that the difference between the pressing pressure of 400 and 500 MPa is significant and, despite the presence of a large number of through-pores, it does not favor their disappearance in the sinters compacted with lower pressure during sintering. An additional beneficial factor used during sintering is nitrogen atmosphere. Previously unpublished research by the team of authors revealed that silver sinters much better in nitrogen atmosphere and, with its high content in the material, it swells much less than in hydrogen atmosphere.

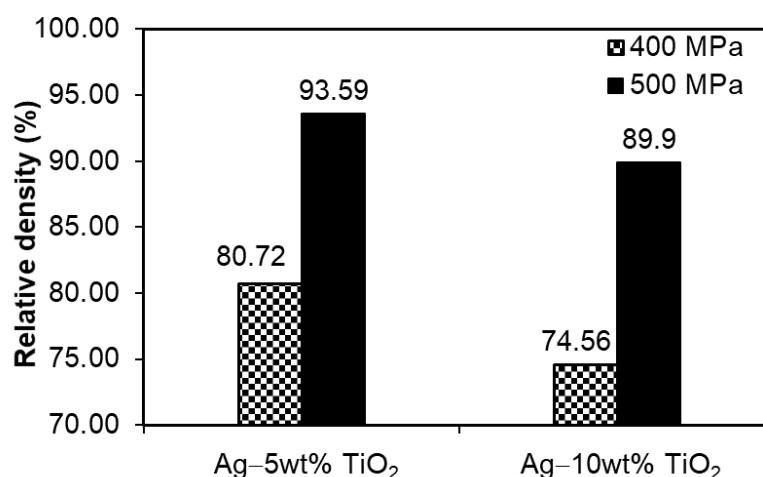


Figure 3. Relative densities of as-sintered PM silver matrix composites depending on chemical composition and process parameters (Archimedes method).

As expected, the addition of TiO_2 lowers the electrical conductivity of the tested materials, both in relation to solid copper and to silver pressed and produced under the same conditions (Table 1). The study shows that the content of the non-metallic phase is more important than the density obtained as a result of the production process. On the one hand, owing to the addition of TiO_2 , the electrical conductivity decreases, but, on the

other hand, the hardness increases in relation to pure silver (Figure 4a), which significantly expands the possibilities of using such materials, e.g., in contacts operating in the start–stop cycle requiring higher hardness of contact surfaces. Increasing the TiO₂ addition content does not increase the hardness. This is due to its distribution in the microstructure in the form of agglomerates and the higher porosity of these materials, which is the result of the increased content of the hard phase on the course of the pressing process, regardless of the pressure applied. Contrary to the hardness, the addition of the TiO₂ reinforcing phase reduces the flexural strength (Figure 4b) and its effect is much greater than the porosity present in the sinters pressed at the pressure of 400 MPa. This is due to the way it is distributed on the boundaries of the silver particles, usually in the form of clusters, which facilitates the propagation of cracks through these areas.

Table 1. Electrical conductivity of Ag–xTiO₂ composites.

Material	Electrical Conductivity, MS/m	Electrical Conductivity, % IACS
Ag	45.9	79.2
Ag-5 wt% TiO ₂ 400 MPa	32.6	56.2
Ag-5 wt% TiO ₂ 500 MPa	35	60.3
Ag-10 wt% TiO ₂ 400 MPa	18.4	31.8
Ag-10 wt% TiO ₂ 500 MPa	19.4	33.4

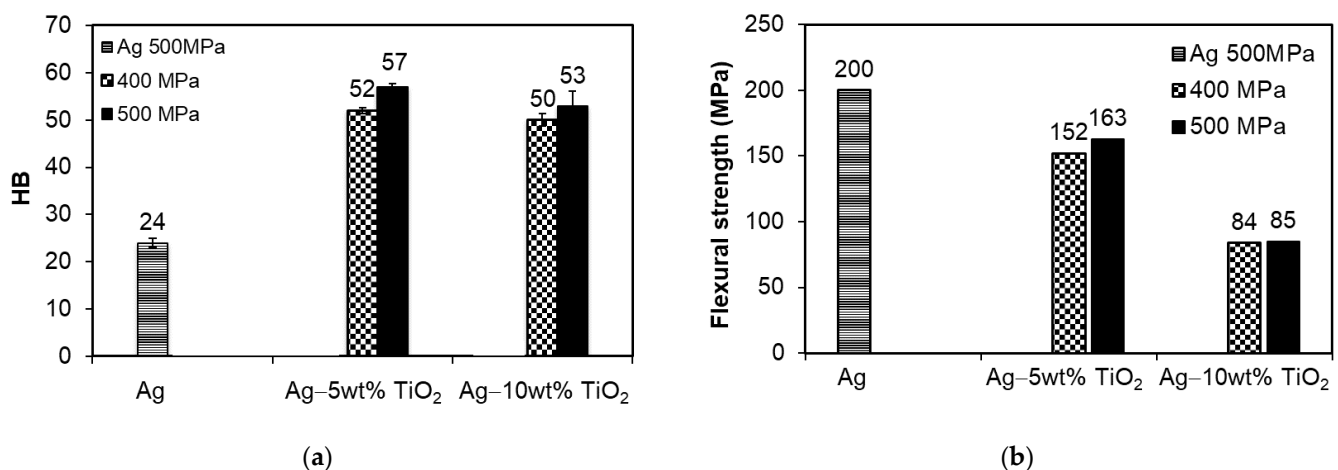


Figure 4. Results of testing composite properties: (a) Brinell hardness; (b) flexural strength.

The microstructure of the investigated materials (Figure 5) consists of areas of silver with single fine-grained TiO₂ particles or clusters arranged on the boundaries. Fine pores are located locally at the interface between the silver particles themselves, as well as between the silver particles and clusters of TiO₂. The observations of the microstructures confirmed that the applied milling is not sufficient to break down entirely all the clusters of TiO₂ particles. The size of these clusters depends on the content of the reinforcing phase and their presence results from the tendency of fine powders to agglomerate, in addition to the difficulty of breaking these agglomerates at the stage of mixing the powders. The use of mixing balls only partially reduced the size of the agglomerations. Nevertheless, the observations with the scanning microscope and transmission electron microscopy confirm the good connection between the matrix and the reinforcing phase as well as the high coherence in the TiO₂ clusters. A detailed analysis of the TiO₂ regions reveals structural changes within its particles.

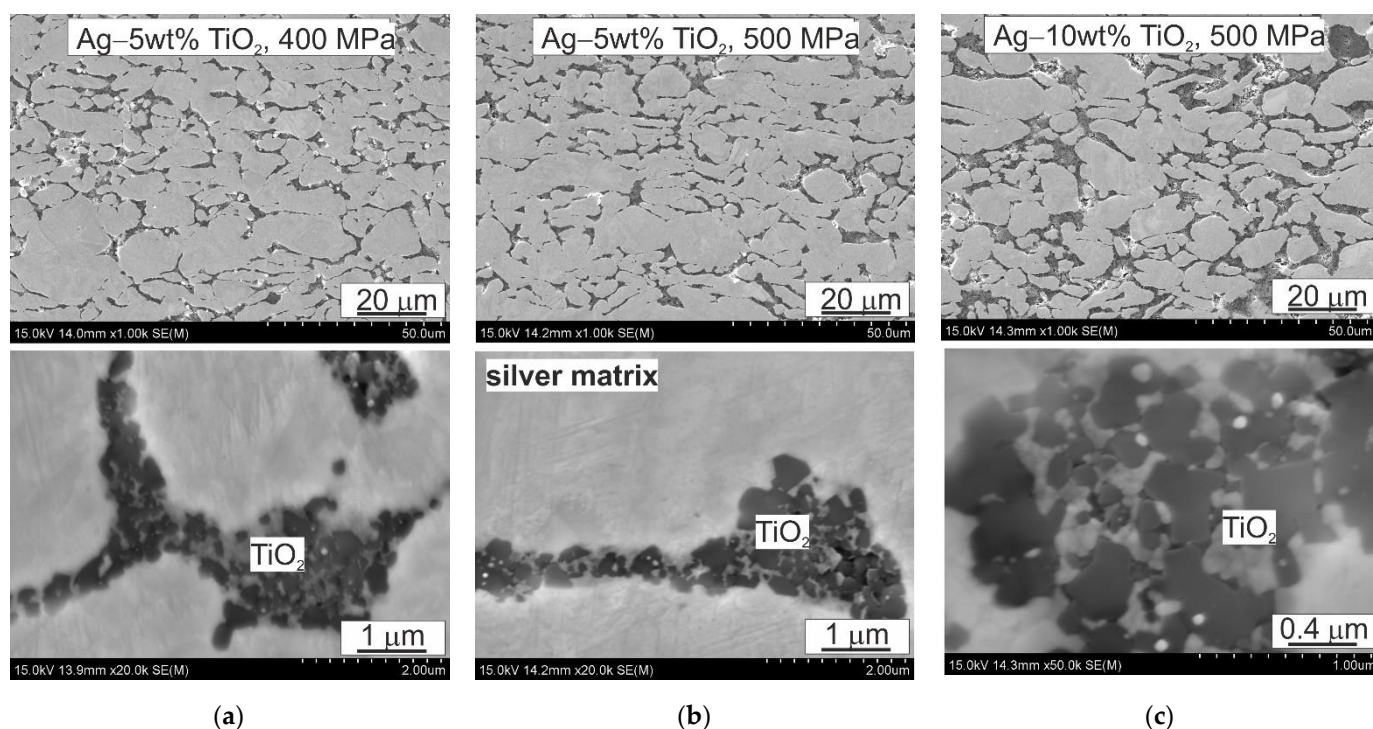


Figure 5. Composite microstructures: (a) Ag-5 wt% TiO₂, $p = 400$ MPa; (b) Ag-5 wt% TiO₂, $p = 500$ MPa; (c) Ag-10 wt% TiO₂, $p = 500$ MPa; SEM.

The results of the chemical composition analysis by the WDS method indicate the diffusion of nitrogen into the area of the TiO₂ reinforcing phase (Figure 6). The presence of Ag₃N or AgN₃ compounds was not found—the process was carried out under conditions that do not favor the formation of these compounds. The studies did not confirm the formation of Ti_xN compounds either, despite the high affinity of titanium for nitrogen. The X-ray studies, the results of which are shown in Figure 7, showed the presence of a new AgTi₃ phase which, after analyzing the element distribution maps, was located inside the TiO₂ additive clusters, but close to the contact boundary with the silver matrix. This indicates the possibility of the release of metallic titanium, probably coming from the TiO₂ particles, which, when analyzed by WDS, reveal oxygen-depleted areas inside. There is also the possibility of nitrogen diffusing inside the TiO₂ particles from the sintering atmosphere in the titanium oxide reduction, leading to the formation of both the AgTi₃ phase and nanometric silver oxide precipitates at the Ag-TiO₂ interface, which results from the local excess oxygen in these areas and the sintering temperature, perhaps favoring its creation. This fact is confirmed by the observation and analysis of the chemical composition of these areas using TEM (Figure 8). The detailed analysis of the intensity peaks for TiO₂ in Figure 7b suggests that some of it was converted to rutile at the sintering temperature and is consistent with the information on anatase, which is stable up to temperatures of around 800 °C.

In order to more fully verify the microstructure of the investigated composites, and, in particular, the bond of the silver matrix with the hard particles of the TiO₂ reinforcing phase, observations of the microstructure were carried out using a transmission electron microscope. Selected results are presented in Figures 8 and 9. In the silver matrix, against the background of cellular dislocation systems, deformation twins are present, which are visible in the form of bands of various widths not exceeding 100 nanometers and high dislocation density (Figure 8a,b). In metals with a face-centered cubic crystal structure, mechanical twinning is favored, among others, by the low stacking fault energy value of silver. In the case of the tested composites, the deformation twins probably arose during pressing and did not disappear despite sintering for 1 h at a temperature above the recrystallization temperature due to the presence of the hard TiO₂ particles in the microstructure. The

presence of the hard reinforcing phase particles prevents microstructure renewal processes, which favors a large accumulation of dislocations in the matrix area and the formation of characteristic twins in the form of bands. In addition, deformation twins are obstacles during dislocation slip, owing to which the matrix is characterized by a high dislocation density. The observations also confirmed the fact that a good bond of the silver matrix with the hard TiO_2 phase was obtained and the local presence of nanometric silver oxide precipitates and AgTi_3 precipitates were found, the growth of which was directed from the silver surface to the interior of the cluster located in this area (Figures 8c,d and 9a,b). The presence of a strongly defective matrix around the presence of TiO_2 particles and the increase in interfacial surfaces as a result of introducing the reinforcing phase will also act as a barrier to the movement of electrons, thus justifying the decrease in electrical conductivity for composites with a higher content of reinforcement in relation to silver.

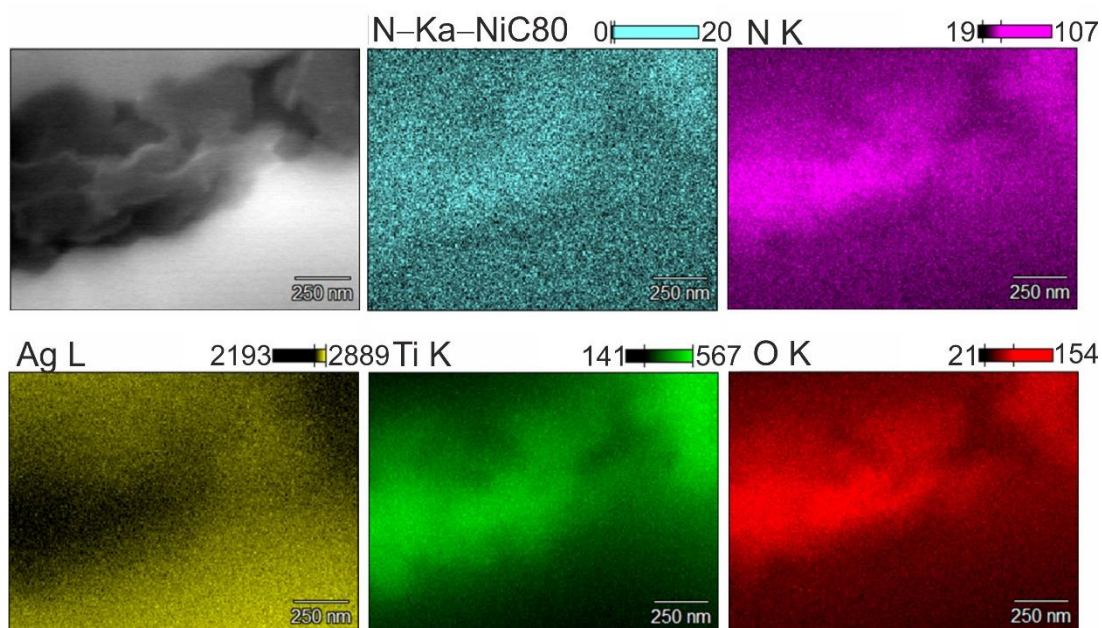


Figure 6. SEM and corresponding WDS mapping micrographs.

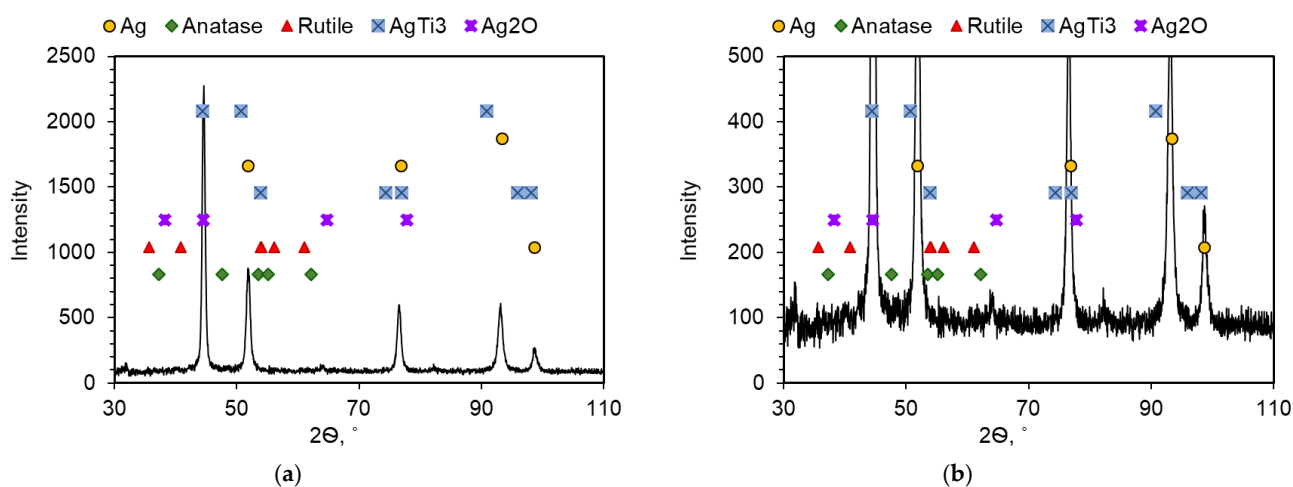


Figure 7. XRD analysis of Ag-5 wt% TiO_2 composites; (a) in range of intensity 0–2500; (b) in range of intensity 0–500.

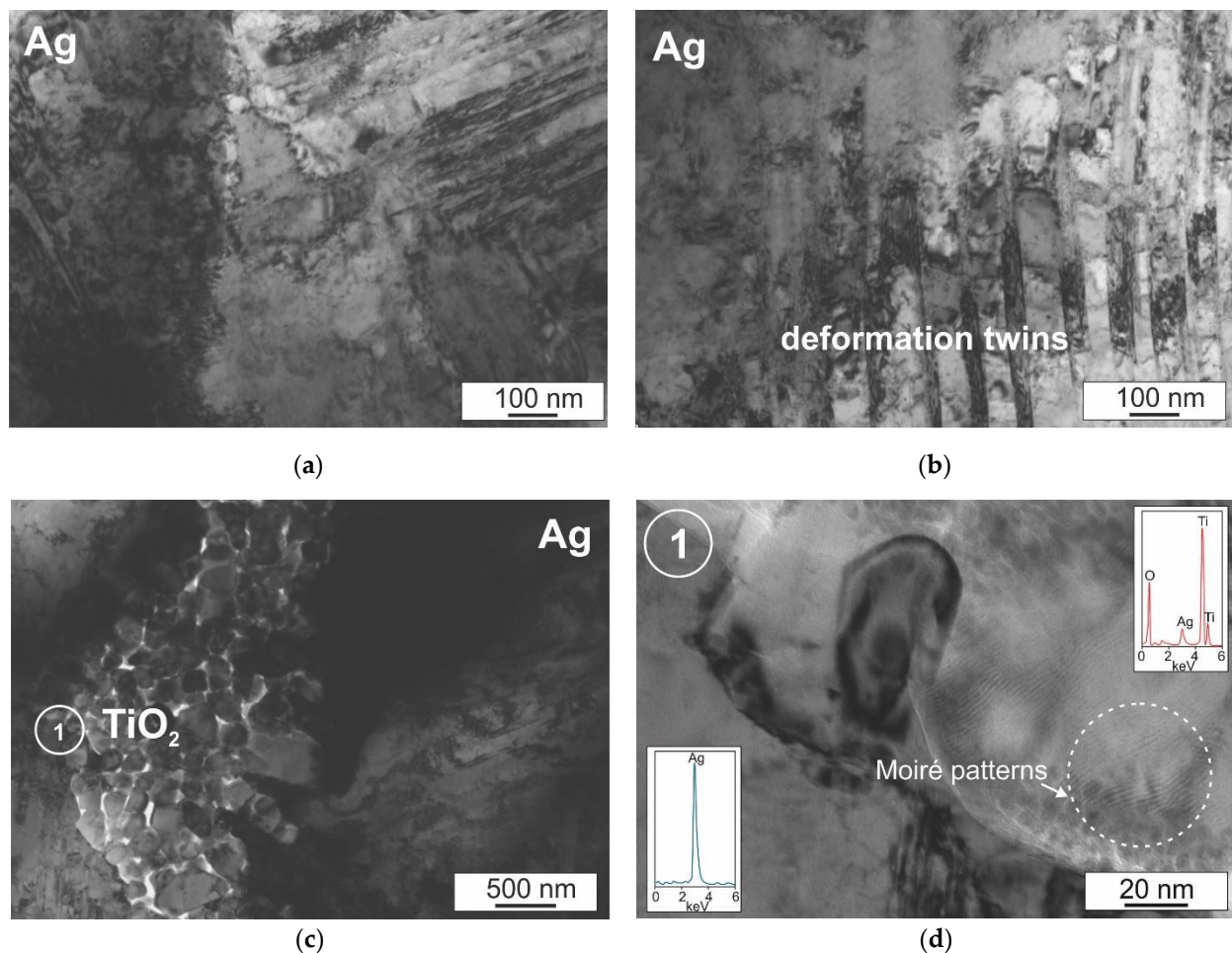


Figure 8. Microstructure of as-sintered Ag–5 wt% TiO₂ composite, $p = 500$ MPa; (a,b) matrix; (c,d) Ag–TiO₂ region; TEM.

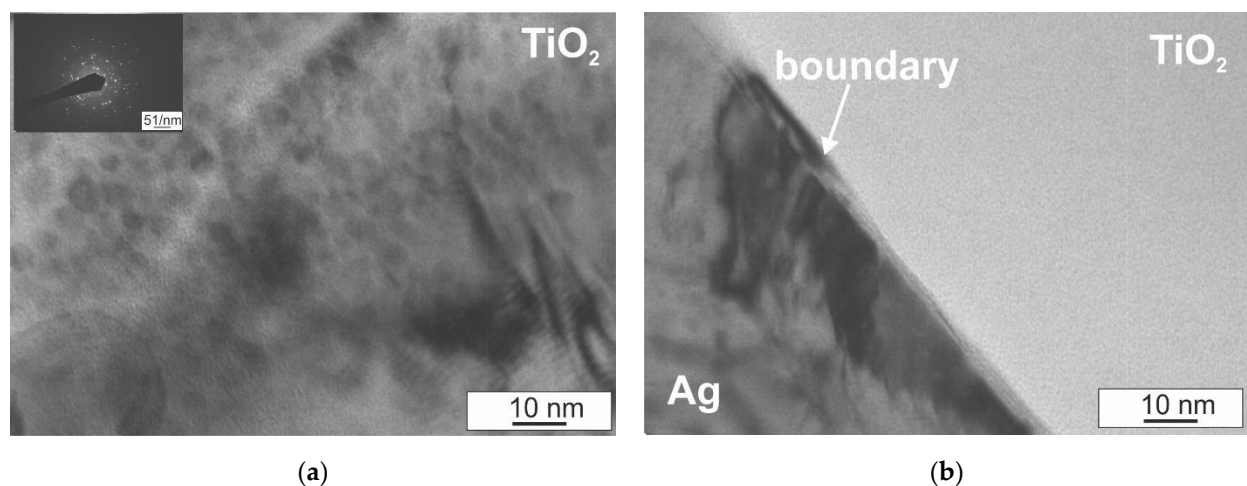


Figure 9. Microstructure of as-sintered Ag–TiO₂ composite, $p = 500$ MPa; (a) TiO₂; (b) boundary between silver matrix and TiO₂ reinforcing phase; TEM.

Moiré patterns are also locally visible within the TiO₂ particles (Figures 8d and 9a), observed as parallel lines, formed by the interference of diffractive lattice planes, which overlap and may have different distances and/or orientations. Moiré patterns are produced by the superposition of two lattices with very small or equal spacings having a suitable mutual orientation [25].

The presence of a large number of defects, in addition to the reinforcing phase, is a component of the reinforcement of composites.

4. Conclusions

The conducted tests allowed the following conclusions to be formed:

- The applied conditions for the production of Ag-xTiO₂ composites by means of powder metallurgy technology made it possible to obtain composites with a density exceeding 90%.
- The addition of TiO₂ significantly reduces the electrical conductivity of the investigated materials, most strongly with the content of 10%, while improving the hardness of the composite, increasing the application possibilities of this type of material.
- Nitrogen, easily diffusible in the sintered material, can cause the appearance of free titanium (as a result of reduction), which reacts with silver to form AgTi₃, and free oxygen atoms, together with silver from the matrix, form nanometric oxide, which locates on the border between silver and TiO₂.

Author Contributions: Conceptualization, B.L.-M. and M.M.; methodology, B.L.-M., M.M., A.W.; investigation, B.L.-M., M.M. and A.W.; writing—original draft preparation, B.L.-M., M.M. and A.W.; writing—review and editing, B.L.-M., M.M. and A.W.; visualization, B.L.-M., M.M. and A.W. All authors have read and agreed to the published version of the manuscript.

Funding: This research was funded by the Polish State Committee for Scientific Research, grant number 16.16.180.006.

Institutional Review Board Statement: Not applicable.

Informed Consent Statement: Not applicable.

Data Availability Statement: Data sharing not applicable.

Acknowledgments: The authors would like to acknowledge Piotr Noga (UST-AGH, Faculty of Non-Ferrous Metals) for support concerning WDS investigations.

Conflicts of Interest: The authors declare no conflict of interest.

References

1. Singh, C.D.H.; Singh Brar, G.; Kumar, H.; Aggarwal, V. A review on metal matrix composite for automobile applications. *Mater. Today Proc.* **2021**, *43*, 320–325. [[CrossRef](#)]
2. Gao, L.; Gan, W.; Xiao, S.; Zhan, X.; Li, J. A robust superhydrophobic antibacterial Ag-TiO₂ composite film immobilized on wood substrate for photodegradation of phenol under visible-light illumination. *Ceram. Int.* **2016**, *42*, 2170–2179. [[CrossRef](#)]
3. Saba, F.; Zhang, F.; Liu, S.; Liu, T. Reinforcement size dependence of mechanical properties and strengthening mechanisms in diamond reinforced titanium metal matrix composites. *Compos. Part B Eng.* **2019**, *167*, 7–19. [[CrossRef](#)]
4. Su, W.; Wei, S.; Hu, S.; Tang, J. Preparation of TiO₂/Ag colloids with ultraviolet resistance and antibacterial property using short chain poly-ethylene glycol. *J. Hazard. Mater.* **2009**, *172*, 716–720. [[CrossRef](#)]
5. Wieczorek, J.; Maciąg, T.; Kowalczyk, K.; Migas, D. Evaluation of thermal properties of MMCp composites with silver alloy matrix. *J. Therm. Anal. Calorim.* **2020**, *142*, 175–182. [[CrossRef](#)]
6. Khalil-Abad, M.S.; Yazdanshenas, M.E. Superhydrophobic antibacterial cotton textiles. *J. Colloid Interface Sci.* **2010**, *351*, 293–298. [[CrossRef](#)]
7. Wieczorek, J.; Oleksiak, B.; Łabaj, J.; Węcki, B.; Mańka, M. Silver matrix composites—Structure and properties. *Arch. Metall. Mater.* **2016**, *61*, 323–328. [[CrossRef](#)]
8. Rigou, V.I.; Marginean, G.; Frunzaverde, D.; Campian, C.V. Silver based composite coatings with improved sliding wear behavior. *Wear* **2012**, *290–291*, 61–65. [[CrossRef](#)]
9. Chang, S.Y.; Lin, J.H.; Lin, S.J.; Kattamis, T.Z. Processing copper and silver matrix composites by electroless plating and hot pressing. *Metall. Mater. Trans. A* **1999**, *30*, 1119–1136. [[CrossRef](#)]
10. Mohsen Momeni, M.; Zeinali, P. Fabrication of Ag electrodeposited-iron doped TiO₂ nanotube composites for photoelectrochemical cathodic protection applications. *J. Electroanal. Chem.* **2021**, *891*, 115283. [[CrossRef](#)]
11. Ranti Oke, S.; Eso Falodun, O.; Mahlatse, M.R.; Ige, O.O.; Olubambi, P.A. Investigation on densification and microstructure of Al-TiO₂ composite produced by Spark plasma sintering. *Mater. Today Proc.* **2019**, *18*, 3182–3188. [[CrossRef](#)]
12. Findik, F.; Uzun, H. Microstructure, hardness and electrical properties of silver-based refractory contact materials. *Mater. Des.* **2003**, *24*, 489–492. [[CrossRef](#)]

13. Hao, X.; Wang, X.; Zhou, S.; Zhang, H.; Liu, M. Microstructure and properties of silver matrix composites reinforced with Ag-doped Graphene. *Mater. Chem. Phys.* **2018**, *215*, 327–331. [[CrossRef](#)]
14. Pontoreau, M.; Thomas, B.; Le Guen, E.; Bourda, C.; Kraiem, N.; Andrey, L.; Silvain, J.F. Synthesis of composite powders composed of silver and carbon nanotubes by liquid-phase reduction method. *Nano-Struct. Nano-Object* **2020**, *24*, 100622. [[CrossRef](#)]
15. Chang, S.Y.; Lin, S.J.; Flemings, M.C. Thermal expansion behavior of silver matrix composites. *Metall. Mater. Trans. A* **2000**, *31*, 291–298. [[CrossRef](#)]
16. Sun, Y.; Wang, Y.; Li, Y.; Zhou, K.; Zhang, L. Tribological behaviors of Ag–graphite composites reinforced with spherical graphite. *Trans. Nonferrous Met. Soc. China* **2020**, *30*, 2177–2187. [[CrossRef](#)]
17. Pratheesya, T.; Harish, S.; Navaneethan, M.; Sohila, S.; Ramesh, R. Enhanced antibacterial and photocatalytic activities of silver nanoparticles anchored reduced graphene oxide nanostructure. *Mater. Res. Express* **2019**, *6*, 074003. [[CrossRef](#)]
18. Wang, Y.W.; Chen, C.W.; Hsieh, J.H.; Tseng, W.J. Preparation of Ag/TiO₂ composite foams via Pickering emulsion for bactericide and photocatalysis. *Ceram. Int.* **2017**, *43*, S797–S801. [[CrossRef](#)]
19. Ko, S.; Banerjee, C.K.; Sankar, J. Photochemical synthesis and photocatalytic activity in simulated solar light of nanosized Ag doped TiO₂ nanoparticle composite. *Compos. Part B* **2011**, *42*, 579–583. [[CrossRef](#)]
20. Zhang, F.J.; Chen, M.L.; Oh, W.C. Photoelectrocatalytic properties of Ag-CNT/TiO₂ composite electrodes for methylene blue degradation. *New Carbon Mater.* **2010**, *25*, 348–356. [[CrossRef](#)]
21. Koo, Y.; Littlejohn, G.; Collins, B.; Yun, Y.; Shanov, V.N.; Schulz, M.; Pai, D.; Sankar, J. Synthesis and characterization of Ag–TiO₂–CNT nanoparticle composites with high photocatalytic activity under artificial light. *Compos. Part B* **2014**, *57*, 105–111. [[CrossRef](#)]
22. Liang, R.; Schneider, O.M.; Lun, N.; Enrique, P.D.; Saha, D.C.; Li Chun Fong, L.C.M.; Jaciw-Zurakowsky, I.; Servos, M.R.; Peng, P.; Zhou, N.Y. Concurrent photocatalytic degradation of organic contaminants and photocathodic protection of steel Ag–TiO₂ composites. *Materialia* **2018**, *3*, 212–217. [[CrossRef](#)]
23. Kawakami, H.; Ilola, R.; Straka, L.; Papula, S.; Romu, J.; Hanninen, H.; Mahlberg, R.; Heikkila, M. Photocatalytic activity of atomic layer deposited TiO₂ coatings on austenitic stainless steels and copper alloys. *J. Electrochem. Soc.* **2008**, *155*, C62–C68. [[CrossRef](#)]
24. Koli, D.K.; Agnihotri, G.; Purohit, R. Properties and characterization of Al–Al₂O₃ composites processed by casting and powder metal-lurgy routes (review). *J. Latest Trends Eng. Technol.* **2013**, *2*, 486–496.
25. Tu, J.F. TEM nano-moiré pattern analysis of a copper/single walled carbon nanotube nanocomposite synthesized by laser surface implanting. *C* **2018**, *4*, 19. [[CrossRef](#)]